

Analysis of Conventional and Novel Delay Lines: A Numerical Study

Omar M. Ramahi

Mechanical Engineering Department, Electrical and Computer Engineering Department,
and CALCE Electronic Products and Systems Center

2181 Glenn L. Martin Hall

A. James Clark School of Engineering

University of Maryland

College Park, MD 20742, U.S.A.

oramahi@calce.umd.edu

www.enme.umd.edu/EMCPL/

Abstract

Delay lines are convenient circuit elements used to introduce delay between circuit board components to achieve required timing. Serpentine or meander lines are the most common of delay lines. These lines introduce delay but also introduce spurious dispersion that makes the signal appear as if it is arriving earlier than expected. The cause of such spurious speed-up or skew is analyzed qualitatively. Previous work found that owing to the periodicity inherent in the serpentine line structure, the crosstalk noise accumulates *synchronously*, thus creating a higher potential for triggering false logic. Numerical simulations are performed using the Finite-Difference Time-Domain (FDTD) method to corroborate the qualitative prediction with physical behavior. Based on the understanding of the coupling mechanism in periodic serpentine lines, a qualitative prediction can be made of the behavior of novel delay lines such as the spiral line. A new delay line, the *concentric Cs* delay lines, is introduced. The design of the new line is based on forcing the crosstalk noise to spread over time, or to accumulate *asynchronously*, thus enhancing the integrity of the received signal.

Key Words: Delay Lines, Serpentine Lines, Meander Lines, Spiral Lines, FDTD, Numerical Simulation, Crosstalk Noise.

I. Introduction

It can be argued that timing problems are amongst the most serious plaguing high-speed digital circuit-board design. As the clock speed increases, the wavelength shrinks. For instance, for a clock speed of 1.5 GHz, the pulse harmonics containing sufficient energy reach beyond 10 GHz, making a typical motherboard or daughter cards electrically

large. As a consequence, a delay line used to introduce precise delay (based on the length of the line and board material) between circuit board elements can no longer be considered to have TEM or quasi-TEM propagation behavior, and to be electromagnetically isolated from neighboring lines that fall within its proximity. With the timing budget shrinking to the picosecond regime, any non-predictable behavior of delay lines can potentially cause a timing imbalance at the receiver end.

Two mechanisms are employed to achieve required signal delay between circuit components. The first is achieved through internal electronic circuitry. The second mechanism, which is the most common and least expensive, is achieved through meandering a transmission line as shown in Fig. 1. The meandered line, commonly referred to as the serpentine line, consists of a number of closely packed transmission line segments. The only objective from meandering the line is to achieve high density (of transmission line) per square inch of circuit board while obtaining signal delay that is directly proportional to the length of the line.

When serpentine lines are used in high-speed digital circuit applications, the time delay through a single serpentine line can be much longer than the rise time of the signal pulse. Under such conditions, serpentine lines have been found to introduce a dispersion that makes the signal *appear* as if it is arriving earlier than would be expected based on the exact electrical length of the line [1]. This spurious speed-up in the signal can be characterized as a type of dispersion. This dispersion is primarily caused by the topology of the line and is directly related to the crosstalk between the adjacent transmission line sections. More specifically, the dispersion is related to two fundamental geometrical parameters: the first

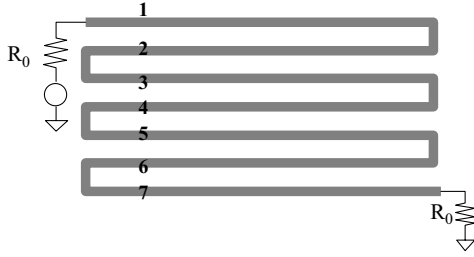


Fig. 1. A matched seven-section serpentine delay line. The Characteristic impedance of each identical section is R_0 .

is the length of each serpentine section, and the second is the spacing between adjacent sections, which influences the capacitive and inductive coupling [1], [2].

Based on these findings, Wu and Chao introduced the flat spiral delay line to force the crosstalk noise to accumulate *asynchronously* [3]. The flat spiral line is distinguished from the classical spiral delay line, which requires three-dimensional topology and therefore cannot be printed on a single board layer. In this work, the flat spiral line will be referred to as the spiral line.

The spiral delay line is considered a significant improvement over the serpentine line. In [3], the motivation behind the spiral line was introduced and analysis was given based on the wave-tracing technique which did not take into account higher-order mode coupling and corner effects. Also in [3], quantitative analysis was also performed to include the effects of multiple and feedback couplings between lines. To incorporate high-order effects into the modeling of serpentine line, especially the coupling between the non-orthogonal lines, the three-dimensional Finite-Difference Time-Domain (FDTD) method was used to analyze serpentine and spiral lines [4]. In a subsequent work, the FDTD method was used to analyze the spiral line for Gaussian pulse excitation [5]. More recently, the Method of Moments (MoM) was used to present a full-wave model for the serpentine line including physical losses [6].

In this work, we use the same qualitative wave-tracing methodology that was adopted in [2] to analyze the spiral line. We show that the wave-tracing methodology can only give qualitative analysis of the line and that a full-wave model is needed to accommodate the effect of corners and

coupling between non-orthogonal segments. We use the FDTD method to analyze the spiral line and show that more inclusive performance can be predicted. Based on the qualitative insight gained from the analysis of the serpentine and spiral line, we introduce a new delay line that we refer to as the *concentric Cs* delay line. Qualitative analysis of the new lines is given followed by full-wave three-dimensional simulation.

The organization of this paper is as follows. In section 2, the mechanism of coupling between two transmission lines is introduced with application to serpentine lines. Sections 3 and 4 present a qualitative analysis followed by full-wave numerical simulation of practical real-world structures for the serpentine and spiral lines, respectively. Section 5 introduces the Concentric Cs delay lines. We note that the FDTD method will be used purely as a numerical simulation tool without giving details of the simulation parameters involved such as the cell size and time step, ...etc. The paper concludes with critical observations that can be used in the design of predictable-delay lines.

II. Weak Coupling Crosstalk

a. Analysis

A typical serpentine delay line is composed of transmission line sections closely packed as shown in Fig. 1. Let us isolate two adjacent sections as shown in Fig. 2. After examination, we notice that the two isolated sections resemble the simplest case of two parallel transmission lines [2]. After ignoring higher-order effects, the two-segment serpentine line shown in Fig.2 is equivalent to the two transmission lines matched at both ends and shown in Fig. 3. Once this observation is made, using conventional transmission line analysis, one can predict the crosstalk induced on the second line due to the launched signal on the first line.

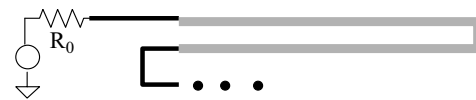


Fig. 2. Segment of a serpentine line.

Considering Fig. 3, the near-end crosstalk, shown as voltage V_2 , is proportional to the mutual capacitance and mutual inductance characterizing the two lines. The coupling coefficient k_{NE} is given by

$$k_{NE} = \frac{1}{4} \left\{ \frac{|C_{12}|}{C_{22}} + \frac{L_{12}}{L_{22}} \right\} \quad (1)$$

where the crosstalk at the near end is given by

$$V_{NE}(t) = k_{NE} [V_A(t) - V_A(t - 2t_d)] \quad (2)$$

where C_{11} and L_{11} are the self capacitance and self inductance, respectively, of the lines, and C_{12} and L_{12} are the mutual capacitance and mutual inductance, respectively, of the coupled lines [1]. Let us assume that the rise time is smaller than the line delay, t_d . If a step function is launched on line 1, then the crosstalk at the near end of line 2 will be a pulse with a duration twice the line delay (i.e., equivalent to the round-trip time t_d). The crosstalk at the far end has a much smaller duration and it equals zero when the capacitive and inductive coupling coefficients are equal (as in the case when the medium is homogeneous as in strip lines) [1]-[2]. Since the pulse on the active line propagates to the right, the voltage at the near end of the passive line is in effect due to a leftward propagating wave. Similarly, the voltage at the far end of the passive line is the accumulation of a rightward propagating wave (which is zero in the case of homogeneous medium).

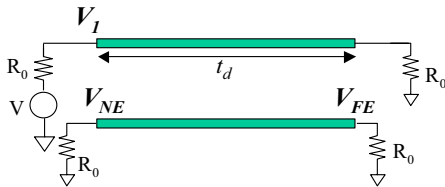


Fig. 3. Parallel transmission lines with matched terminations. A pulse transmitted on the upper line generates crosstalk on the lower line that propagates in a manner equivalent to the case of the serpentine line segment shown in Fig. 2.

If line 1, in Fig. 3, is excited by a pulse starting at $t = t_0$ and of duration T assumed to be shorter than the length of the line t_d , then the near-end crosstalk will consist of two opposite polarity pulses separated by $2t_d - T$, and each of duration T . This can be shown using the principle of superposition. By decomposing the finite duration input pulse into two opposite polarity step functions separated by T , the near-end crosstalk will be the sum of two pulses. The first pulse will have positive polarity and is excited at time t_0 . The second pulse will have negative polarity and will start at time $t_0 + T$. The sum of the two pulses yields a waveform consisting of two pulses, each of duration T and separated by a time interval of width $2t_d - T$.

To demonstrate these two scenarios, we use the FDTD method to simulate the behavior of two parallel strip lines (similar topology to Fig. 3) with cross section shown in Fig. 4.

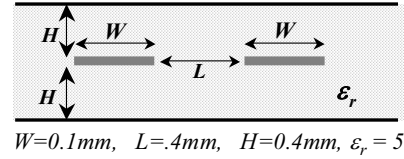


Fig. 4. Strip line cross section.

Figure 5 shows the near-end voltages on the active and passive lines when the excitation is a step function. The far-end voltage at the active line is also shown in Fig. 5. One can observe that the duration of the near-end crosstalk is T .

Figure 6(a) shows the near-end voltage on the active and passive lines when the excitation is a pulse of duration 250 picoseconds. We observe that the near-end passive line experiences two opposite polarity pulses, each of the same duration as the original pulse. This performance is in full agreement with our earlier prediction. For completion, we show the far-end voltage on the active and passive lines in Fig. 6(b). Notice that the bump appearing in Fig. 5 is due primarily to the numerical dispersion of the FDTD method and the physical dispersion caused by the propagation in the strip line configuration.

When forming a serpentine line by closely connecting identical transmission line sections, a similar crosstalk mechanism to that discussed above takes effect, except now one should also account for coupling between non-orthogonal lines and the coupling between orthogonal line segments. Let us consider the serpentine line composed of seven transmission line segments (shown in Fig. 1). Suppose V_{in} is a step voltage with a magnitude of one volt.

Once this voltage waveform is launched at the transmitter end, a voltage of magnitude $1/2$ appears on line 1. The voltage at line 1 will induce leftward traveling waves at the near ends of lines 2, 4 and 6. These signals continue to travel on lines 3, 5 and 7 respectively. Notice that the launched signal does not excite any forward propagating waves on any of the lines as per the discussion given above. (Throughout this work, forward propagating cross talk refers to crosstalk propagating towards the receiver. Similarly,

“backward propagating crosstalk refers to crosstalk propagating towards the source.)

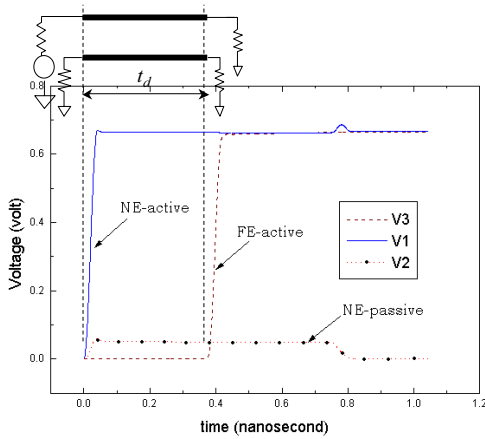


Fig. 5. Wave forms on the active and passive lines due to a step function excitation. V1 is the input pulse at the active line, V2 is the near-end voltage at the passive line, and V3 is the far-end voltage at the active line.

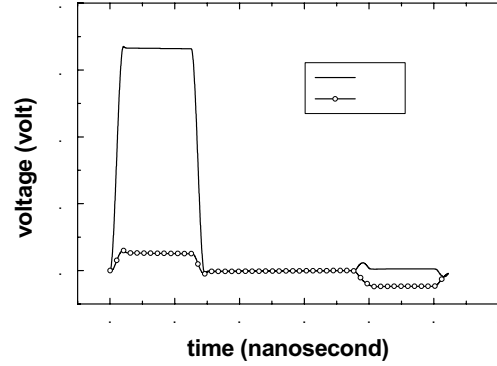
Assuming that multiple coupling is negligible (multiple coupling refers to the feedback crosstalk between lines), equation (1) can be used to find the magnitudes of the crosstalk induced on any line by the main signal as it propagates on any other line. The coupling between any two lines m and n , where $m \neq n$, can be written as

$$k_{|m-n|} = \frac{1}{4} \left\{ \frac{|C_{mn}|}{C_{mm}} + \frac{L_{mn}}{L_{mm}} \right\} \quad (3)$$

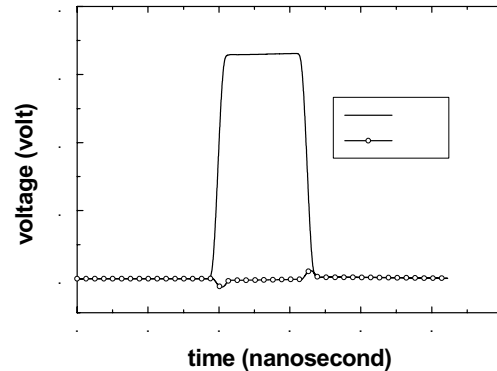
where C_{mm} and L_{mm} are the self capacitance and self inductance, respectively, of line m , and C_{mn} and L_{mn} are the mutual capacitance and mutual inductance, respectively, of the coupled lines m and n . Let us assume that the rise time is much smaller than the pulse width. Let us consider the leftward traveling wave excited at line 2, which has a magnitude of $k_1/2$, and duration $2t_d$. Furthermore, this wave arrives at the receiver end ahead of the main signal by $2t_d$. Similarly, backward traveling waves will appear on lines 4 and 6 having duration of $2t_d$ and magnitudes $k_3/2$ and $k_5/2$ respectively. These signals will arrive ahead of the main signal by $4t_d$ and $6t_d$, respectively.

When the main signal starts to propagate along line 2, it induces forward propagating crosstalk on lines 3, 5 and 7. The magnitudes of these crosstalk signals are $k_1/2$, $k_3/2$ and $k_5/2$, respectively. These

signals arrive ahead of the main signal by $2t_d$, $4t_d$ and $6t_d$, respectively. It is important to realize that as the main signal hops from one line to the next, the crosstalk induced is additive. In other words, the crosstalk noise accumulates *synchronously*. This process of coupling continues until the main signal arrives at the receiver. In fact, by adding the effect of all induced crosstalk, the waveform obtained at the receiver end becomes a laddering waveform, where each of the ladder levels is of duration $2t_d$.



(a)



(b)

Fig. 6. Wave forms on the active and passive sections of a two-line system obtained using the FDTD method. (a) Near-end voltage (NE-a = Near end at active line, NE-p = Near end at passive line). (b) Far-end voltage (FE-a = Far end at active line, FE-p = Far end at passive line).

Therefore, when the seven-section serpentine line (Fig. 1) is excited with a step function starting at t_0 , we can expect the receiving end waveform to have a laddering waveform. When the excitation is a finite duration pulse, then the shape of the received signal will depend on whether T is shorter or longer than the round trip $2t_d$. When T is longer than $2t_d$, the qualitative behavior of the received signal is depicted

in Fig. 7(a), showing degradation of the pulse magnitude once the main signal is received. On the other hand, when T is shorter than $2t_d$, the received waveform consists of a train of pulses, each of duration T and separated by $2t_d - T$, as shown in Fig. 7(b).

The wave tracing analysis adopted here can be further generalized to serpentine lines composed of many sections. It can be shown that for a general serpentine delay line consisting of $2N+1$ sections, a laddering waveform is generated and it arrives before the main signal. The laddering wave includes N ladders; each ladder is of width $2t_d$ and level $ik_{2(N-1)+1}$ for $i=1$ to N .

In light of the above analysis, several observations can be made:

1. The laddering wave creates the impression that the pulse is arriving earlier than intended. In reality, however, the waveform arriving at the receiver is composed of two signals: the crosstalk laddering waveform (noise) and the unadulterated signal.
2. The crosstalk accumulates *synchronously* at the receiving end. The synchronous accumulation is due to the *periodicity* of the serpentine line structure.
3. The highest level of the laddering waveform can reach several times the level of crosstalk induced between two adjacent lines. In fact, the cumulative magnitude can be higher than the level of the main signal.
4. The magnitude of each ladder is proportional to the capacitive and inductive coupling between the lines.
5. The spreading of the laddering wave, i.e., the width of each ladder, is directly proportional to the length of the serpentine line segments.
6. When the pulse duration is greater than $2t_d$, where t_d is the delay through one section, the cumulative effect is less pronounced, producing ladders of short duration. The net effect is that the pulse arrives at the receiving end as a dispersed wave with an apparent rise time longer than that of the original signal. In such case, the serpentine line can be interpreted as a low-pass filter.
7. When the pulse duration is smaller than $2t_d$, where t_d is the delay through one section, the received waveform consists of a train of pulses, each of duration T and separated by $2t_d - T$.

b. Numerical Experiments

Several assumptions were made in the wave tracing analysis presented above. These were:

1. Negligible non-adjacent line coupling.
2. The backward propagating crosstalk was assumed to be zero. In the general case of non-homogeneous media, there is some backward induced crosstalk.
3. The small transmission line segments that connect the longer sections (orthogonal sections) have been assumed to have zero delay (zero physical length).
4. Negligible multi-modal propagation.

Considering the above simplifications, the qualitative model discussed earlier serves only to give an understanding of the primary crosstalk contributors. For a more accurate prediction of the performance of the serpentine line, the three-dimensional FDTD method will be used since it fully integrates the constraints listed above.

The first design tested is that of the seven-section serpentine line discussed earlier (see Fig. 1). A cross section of two adjacent lines of this geometry is shown in Fig. 4. The total electrical length of the line is 114.6 mm (4.51 in). The length of each section is 16.6 mm (0.65 in). Figure 8 shows the signal at the receiver end. Comparison is made to the control line. (In all the experiments discussed in this paper, the control line is a straight line with electrical length equivalent to that of the delay line under examination. The length of a delay line is considered to be the length of a line that runs through the center of the line, including bends.)

Observing Fig. 8, we notice that the wave tracing analysis predicted the ladders that precede the main signal only. While such prediction is quite important, it did not account for the unexpected high signal level received after the arrival of the main signal (overshoot). Although the high level occurs beyond the logic-switching instant, nevertheless, it can have an adverse effect when the signal switches to zero as false logic could be triggered.

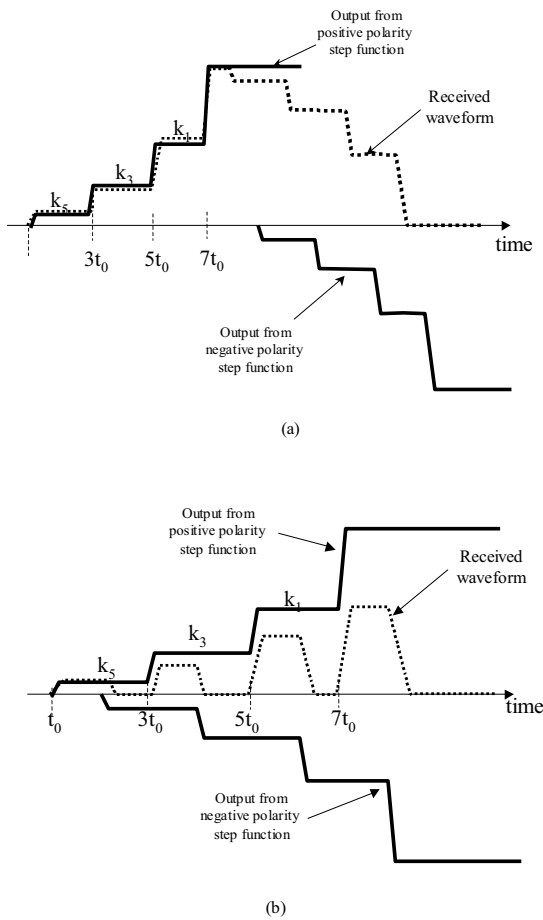


Fig. 7. Wave form at the receiving end of a serpentine line due to a pulse with a duration of T . (a) $T > 2td$. (b) $T < 2td$.

For the second test, we consider a more realistic serpentine line, where the total electrical length of the line is 405.4 mm (15.96 in). Two variations of this line are considered, as shown in Figs. 9 and 10, and will be referred to as Case A and Case B, respectively. The difference between the two topologies considered is that one has shorter sections than the other. Notice that in both cases, the lines have equivalent length, have identical line separation between adjacent segments and both topologies occupy equal board area. The excitation waveform is a pulse having a finite duration of 1.4 nanoseconds and rise time of 100 picoseconds.

Figure 11 shows the response of these two lines in comparison to the reference line. The serpentine line designated as Case B has longer sections and, consequently, its receiver signal had ladders that are

longer than Case A. However, this difference is of minor importance since the low-to-high switching occurs at approximately the same time.

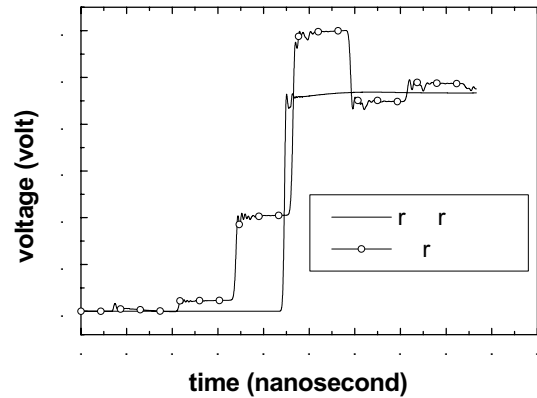


Fig. 8. Received wave form for the seven-section serpentine line.

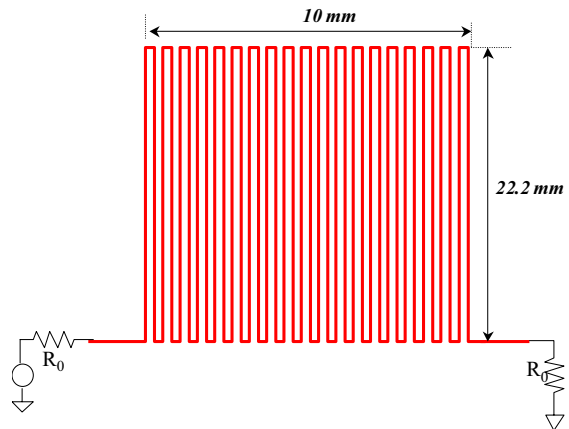


Fig. 9. 19-section serpentine line.

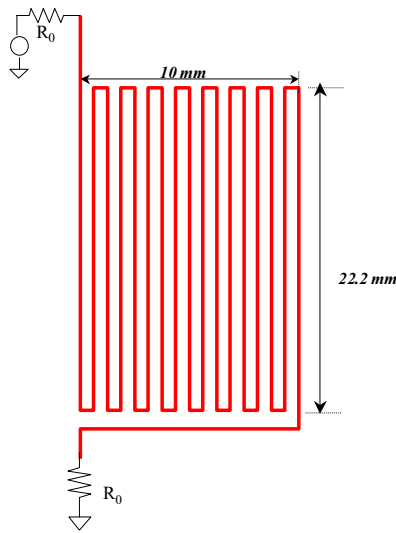


Fig. 10. 17-section serpentine line.

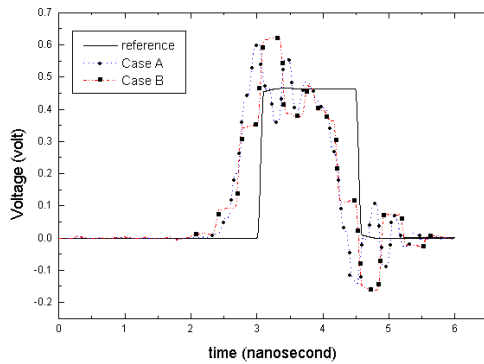


Fig. 11. Response of the 15.96 in long serpentine lines in comparison to the reference line.

III. The Spiral Delay Line

In the serpentine line, the crosstalk was found to accumulate synchronously. This accumulation can be significant enough to trigger false logic. Ideally, this crosstalk needs to be eliminated; however, since the crosstalk is inversely proportional to the separation between the lines, the only way to eliminate or reduce the crosstalk would be to increase the separation between the lines and/or to increase the coupling between the line and the reference plane. Increasing the separation of the segments unfortunately requires larger circuit board area, which can be either expensive, or impossible in light of the density requirements. Therefore, given that for

the transmission line density (or etch density) to remain unchanged, the separation between the lines must not be changed. An alternate design, which forces the crosstalk to accumulate *asynchronously*, was proposed in [3] and is shown in Fig. 12. This alternate design, the flat spiral delay line, minimizes the periodicity in the transmission line routing as much as practicable.

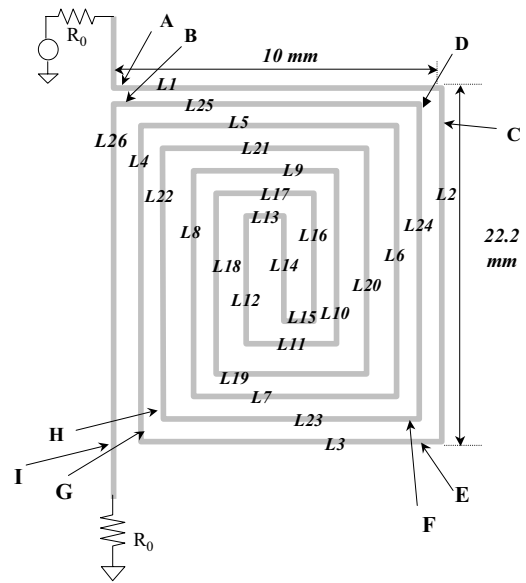


Fig. 12. Spiral delay line.

The most prominent feature of the spiral delay line is the spreading, over time, of the crosstalk noise. To demonstrate how the coupling mechanism works in the spiral line, we will initially assume that coupling between non-adjacent lines is negligible. Let us consider the line shown in Fig. 12, and let us assume that the signal arrives at point A at time $t=0$. Once the signal arrives at A, forward propagating crosstalk is induced at point B. This crosstalk arrives before the main signal by the time delay needed to propagate through the entire length of the line minus the segment L26. In other words, the induced forward propagating crosstalk at B arrives only after the time needed to travel the segment L26. (Henceforth, the time delay through segment LN will be denoted by t_{LN}). So the first crosstalk induced at B by the arrival of the signal at A arrives at $t=t_{L26}$. When the main signal arrives at point C, forward propagating crosstalk is induced at D, arriving at the receiver at approximately $t=t_{L1}+t_{L25}+t_{L26}$.

Similarly, when the main signal arrives at E, it induces at point F a forward crosstalk which arrives

at the receiver at $t = t_{L1} + t_{L2} + t_{L26} + t_{L25} + t_{L24}$. Next, the signal arrives at G, inducing forward propagating crosstalk at H, which arrives in $t = t_{L1} + t_{L2} + t_{L3} + t_{L26} + t_{L25} + t_{L24} + t_{L23}$. However, the signal arriving at H will also induce forward propagating crosstalk at I. The crosstalk induced at I arrives at the receiver at $t = t_{L1} + t_{L2} + t_{L3}$. As the signal propagates further towards the receiver, it continues to induce crosstalk in the adjacent lines.

The above wave-tracing analysis ignores coupling between non-adjacent lines. However, even if this coupling is included, it is easy to see that the crosstalk noise will be distributive and will not accumulate synchronously. When the voltage excitation is a pulse of finite duration, the opposite polarity crosstalk induced by the trailing edge of the excitation pulse will help in reducing the final cumulative crosstalk.

To demonstrate performance of the flat spiral delay line, we construct a line with electrical length, line separation, and total board area, all equal to the serpentine lines shown in Figs. 9 and 10. The cross-section parameters are given in Fig. 4, and the rise time and pulse duration are as before (pulse width of 1.4 nanoseconds and rise time of 100 picoseconds). The dimensions of this spiral line are shown in Fig. 12.

Figure 13 shows the signal at the receiving end of the spiral line in comparison with the control line. The outstanding performance of the spiral line is clearly visible. We observe that the crosstalk noise was spread over time ahead of the main signal resulting in a high fidelity signal. In fact, for the case considered, we notice that the maximum crosstalk stays at or below 10% of the signal level, thus considerably reducing the potential for triggering false logic. We note here that slight shift between the signal due to the control line and the unadulterated signal due to the spiral line is due to a slight difference in line lengths.

The singular feature of the spiral line is its ability to spread the noise over a larger duration. A key observation is that the signal arriving at the receiving end is composed of the unadulterated pulse in addition to the asynchronous noise. This implies that the spiral line can lead to an almost perfect isolation of the accumulative noise from the unadulterated pulse.

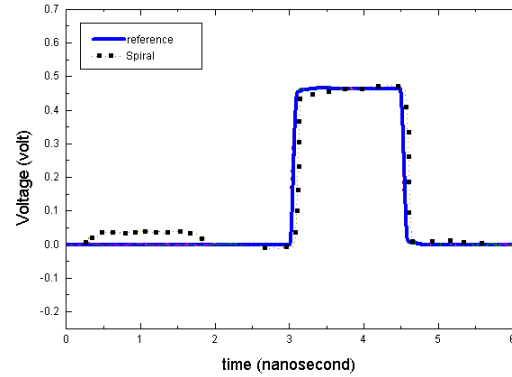


Fig. 13. Response of the 15.96 in long spiral line in comparison to the reference line.

IV. The Concentric Cs Delay Line

From the analysis and simulation of the spiral line, the concept of *asynchronous* coupling is emerging as a powerful mechanism to reduce the apparent dispersion of a delay line. This section introduces a novel design that exploits this mechanism of asynchronous coupling. The new delay line, shown in Fig. 14, will be referred to as the *concentric Cs* delay line. (The name concentric Cs was chosen since this new transmission line resembles different lines shaped as the letter C and centered at one location.) The design of the new line was motivated by the theme of reducing the periodicity in the topology of the structure in order to minimize the accumulative or synchronous coupling.

Using wave-tracing analysis, one can qualitatively predict the performance of the Cs line. Similar to the spiral line, the Cs line distributes the coupling over time. Consider a pulse entering the line at the beginning of section L1 (see Fig. 14). This pulse will induce a crosstalk that will precede the primary (or unadulterated) signal by a time period corresponding to the propagation over segments L1, L2, L3, L4, L5 and L6. Notice that in contrast to the spiral line, this (first-appearing) crosstalk will precede the unadulterated signal by a relatively short period, however, the topology of the Cs line prevents synchronous accumulation. One can qualitatively describe the periodicity in the Cs line structure as lying in between that of the serpentine line and the spiral line. The relative advantage of the mid-level periodicity in the structure becomes more apparent when observing the full-wave behavior as shown below.

To demonstrate the behavior of the Cs line, we design a line, equivalent in electrical length, line spacing and total board area, to the spiral and serpentine lines studied earlier. The dimensions of this design are shown in Fig. 14. Figure 15 presents the result of the FDTD simulation, under previous excitation conditions, showing the signal at the receiver end.

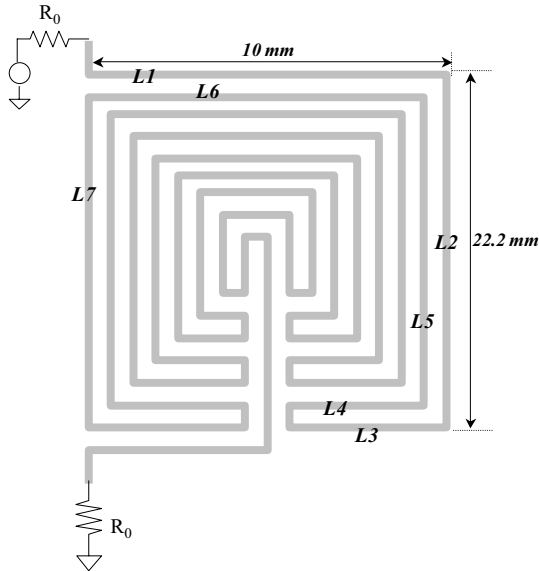


Fig. 14. The concentric Cs delay line.

Comparison is made to the spiral, serpentine and reference lines. Clearly visible from Fig. 15 is the concentration, or accumulation of the noise in the close proximity of the unadulterated signal. We further observe that, for the particular topology and line dimensions considered, that the receiver signal remains at or below 35% of the peak amplitude of the transmitted pulse.

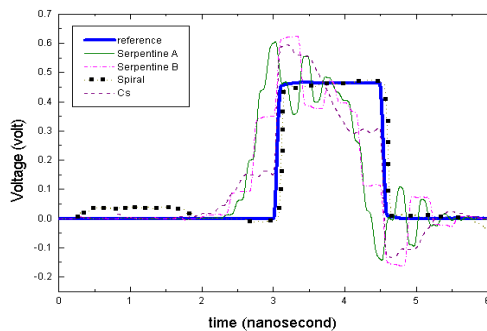


Fig. 15. Response of the concentric Cs line in comparison to the serpentine and spiral lines of equal length.

In comparison to the spiral line, the Cs line keeps the noise closer to the main signal, whereas the spiral line distributes the noise over longer time duration. From this perspective, the spiral line is superior to the Cs line. However, if one were to consider an excitation composed of a train of pulses, as would be the case in practical scenarios, it might be more advantageous to force the crosstalk noise to accumulate closer to the pulse that generates it and not interfere with other pulses.

V. Summary

This paper presented a qualitative analysis of serpentine and flat spiral delay lines based on the simply, yet powerful, ray tracing technique. The three-dimensional FDTD method was used to predict the full-wave performance of these delay lines, thus accounting for higher-order modes, multiple and feedback coupling and the effect of orthogonal segments. Despite the strength and completeness of the FDTD method, the ray tracing method facilitated an understanding of the coupling mechanism in complex-shaped delay lines and lead to the introduction of novel delay line such as the flat spiral line. A new line, the concentric Cs delay line was introduced based on the concept of reducing the periodicity in the structural topology, thus forcing the crosstalk noise to accumulate asynchronously. Numerical simulation using the three-dimensional full-wave FDTD method showed that the new designs result in receiver waveform that is less susceptible to triggering false logic than in the case of the serpentine line.

References

- [1] H. B. Bakoglu, *Circuits, Interconnections, and Packaging for VLSI*, Addison Wesley, Reading, MA, 1990.
- [2] R. B. Wu and F.L. Chao, "Laddering wave in serpentine delay-line," *IEEE Trans. Components Packaging Manufacturing Tech. Part-B Advanced Packaging*, Vol. 18, No. 4, pp. 644-650, Nov. 1995.
- [3] R. B. Wu and F.L. Chao, "Flat spiral delay line design with minimum crosstalk penalty," *IEEE Trans. Components Packaging Manufacturing Tech. Part-B Advanced Packaging*, Vol. 19, No. 2, pp. 397-402, May 1996.
- [4] O. M. Ramahi, "FDTD analysis of conventional and novel delay lines," Presented at the 16th Annual Review of Progress in Applied Computational Electromagnetics meeting, Monterey, CA, March 20-25, 2000.
- [5] N. Orlanovic, R. Raghuram and N. Matsui, "Characterization of microstrip meanders in PCB

interconnects,” Electronic Components and Technology Conference, Conference Proc., May 21-24, 2000.

- [6] B. J. Rubin and B. Singh, “Study of meander line delay in circuit boards,” *IEEE Trans. Microwave Theory Tech.*, Vol. 48, No. 9, pp. 1452-1460, Sept. 2000.



Omar M. Ramahi

received the BS degrees in Mathematics, and Electrical and Computer Engineering (highest honors) from Oregon State University, Corvallis, OR in 1984. He received his M.S. and Ph.D. in Electrical and Computer Engineering in 1986 and 1990, respectively from the University of Illinois at Urbana-Champaign. From 1990-1993, Dr. Ramahi held a visiting fellowship position at the University of Illinois at Urbana-Champaign. From 1993 to 2000, he worked at Digital Equipment Corporation and then Compaq (presently, Hewlett Packard), where he was member of the Alpha Servers Product Development Group. In August of 2000, he joined the faculty of the A. James Clark School of Engineering at the University of Maryland at College Park, as an Assistant Professor in Mechanical Engineering, Assistant Affiliate Professor of Electrical and Computer Engineering, and a Faculty Member of CALCE Electronic Products and Systems Center.

Dr. Ramahi served as a consultant to several companies. He was instrumental in developing computational techniques to solve a wide range of electromagnetic radiation problems in the fields of antennas, high-speed devices and circuits and EMI/EMC. His interests include high-speed devices, packaging, and interconnects, experimental and computational EMI/EMC studies, biomedical applications of electromagnetics, novel optimization techniques, RF MEMS, interdisciplinary studies involving interaction of novel materials and electromagnetic energy, and high-impedance electromagnetic bandgap surfaces. He has authored and co-authored over 120 journal and conference papers and presentations, and has given numerous short courses to the industry. He is a co-author of the book *EMI/EMC Computational Modeling Handbook* (Kluwer Academic, 2nd Ed., 2001). Dr. Ramahi is a member of Eta Kappa Nu, Tau Beta Pi, Senior Member of IEEE and a member of the Electromagnetics Academy.